HOKKAIDO UNIVERSITY

Title	Operando QEXAFS studies of Ni2P during thiophene hydrodesulfurization: direct observation of Ni-S bond formation under reaction conditions
Author(s)	Wada, Takahiro; Bando, Kyoko K.; Miyamoto, Takeshi et al.
Citation	Journal of Synchrotron Radiation, 19(2), 205-209 https://doi.org/10.1107/S0909049512001197
Issue Date	2012-03
Doc URL	https://hdl.handle.net/2115/48653
Type	journal article
File Information	SR19-2_205-209.pdf

Hokkaido University Collection of Scholarly and Academic Papers : HUSCAP

electronic reprint

Journal of
Synchrotron Radiation
ISSN 0909-0495
Editor: **G. Ice**

Operando QEXAFS studies of Ni_2P during thiophene hydrodesulfurization: direct observation of Ni—S bond formation under reaction conditions

Takahiro Wada, Kyoko K. Bando, Takeshi Miyamoto, Satoru Takakusagi, S. Ted Oyama and Kiyotaka Asakura

J. Synchrotron Rad. (2012). **19**, 205–209

Copyright © International Union of Crystallography

Author(s) of this paper may load this reprint on their own web site or institutional repository provided that this cover page is retained. Republication of this article or its storage in electronic databases other than as specified above is not permitted without prior permission in writing from the IUCr.

For further information see http://journals.iucr.org/services/authorrights.html

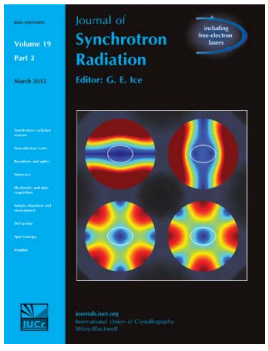

Synchrotron radiation research is rapidly expanding with many new sources of radiation being created globally. Synchrotron radiation plays a leading role in pure science and in emerging technologies. The *Journal of Synchrotron Radiation* provides comprehensive coverage of the entire field of synchrotron radiation research including instrumentation, theory, computing and scientific applications in areas such as biology, nanoscience and materials science. Rapid publication ensures an up-to-date information resource for scientists and engineers in the field.

Crystallography Journals Online is available from **journals.iucr.org**

Journal of
Synchrotron Radiation
ISSN 0909-0495

Received 17 September 2011
Accepted 10 January 2012

Operando QEXAFS studies of Ni_2P during thiophene hydrodesulfurization: direct observation of Ni—S bond formation under reaction conditions

Takahiro Wada,[a,b] Kyoko K. Bando,[c] Takeshi Miyamoto,[a,b] Satoru Takakusagi,[a,b] S. Ted Oyama[d,e] and Kiyotaka Asakura[a,b]*

[a]Catalysis Research Center, Hokkaido University, Kita 21-10, Sapporo 001-0021, Japan, [b]Department of Quantum Science and Engineering, Graduate School of Engineering, Hokkaido University, Kita 21-10, Sapporo 001-0021, Japan, [c]Nanosystem Research Institute, National Institute of Advanced Industrial Science and Technology, 1-1-1 Higashi, Tsukuba, Ibaraki 305-8565, Japan, [d]Department of Chemical Systems Engineering, The University of Tokyo, 7-3-1 Hongo, Bunkyo-ku, Tokyo 113-8656, Japan, and [e]Department of Chemical Engineering and Chemistry, Virginia Polytechnic Institute and State University, Blacksburg, VA 24061-0211, USA. E-mail: askr@cat.hokudai.ac.jp

Structural changes in Ni_2P/MCM-41 were followed by quick extended X-ray absorption fine structure (QEXAFS) and were directly related to changes in X-ray absorption near-edge structure (XANES) which had been used earlier for the study of the active catalyst phase. An equation is proposed to correct the transient QEXAFS spectra up to second-order in time to remove spectral distortions induced by structural changes occurring during measurements. A good correlation between the corrected QEXAFS and the XANES spectral changes was found, giving support to the conclusions derived from the XANES in the previous work, namely that the formation of a Ni—S bond in a surface NiPS phase is involved in the active site for the hydrodesulfurization reaction.

© 2012 International Union of Crystallography
Printed in Singapore – all rights reserved

Keywords: EXAFS; quick-EXAFS; hydrodesulfurization; operando XAFS; Ni_2P.

1. Introduction

Hydrodesulfurization (HDS) catalysts, which reduce sulfur content in transportation fuels, are important in the refining industry. Transition metal phosphides are a new class of HDS catalysts with promising activity (Dhandapani *et al.*, 1998). Among these, Ni_2P has been found to show the highest activity for HDS reactions, especially for refractory compounds such as 4,6-dimethyldibenzothiophene, with activity higher than conventional catalysts like CoMoS or NiMoS on an active site basis (Oyama, 2003). It is a challenging issue to elucidate the active site and reaction mechanism of the highly active Ni_2P. Elemental analysis has shown that a substantial amount of sulfur accumulated in the catalysts in the course of reactions (Oyama *et al.*, 2002; Kim *et al.*, 2005; Sawhill *et al.*, 2005). *In situ* X-ray absorption fine structure (XAFS) is a powerful technique for characterizing catalyst structure during reactions (Bart, 1986; Bart & Vlaic, 1987; Iwasawa, 1996); XAFS is composed of two parts: XANES (X-ray absorption near-edge structure) and EXAFS (extended X-ray absorption fine structure). Kawai *et al.* found a clear oscillation in the difference EXAFS spectra between a sample of Ni_2P/SiO_2 in hydrogen before reaction and the same sample during HDS reaction that could be associated with the formation of a Ni—S bond of length 0.230 nm (Kawai *et al.*, 2006, 2007, 2008). They also found a feature at 8333.3 eV in the XANES region that decreased in intensity in going to steady-state reaction. They attributed the change in the XANES spectrum also to the formation of a Ni—S bond. In order to better elucidate the relationship between the Ni—S bond and the reaction mechanism, time-resolved XAFS studies together with transient product analysis can be a powerful combination. In the past we have carried out such measurements with *in situ* simultaneous time-resolved XANES measurements of the supported Ni_2P, focusing on the changes in the XANES signal, together with *in situ* Fourier transform infrared spectroscopy (FTIR) as well as product analysis (Bando *et al.*, 2009; Oyama *et al.*, 2009). We found that Ni—S bond formation occurred before high activity was observed for the HDS reaction. We concluded that a surface phosphosulfide (NiPS) was the active structure of the Ni_2P catalyst for the HDS reaction (Bando *et al.*, 2009). But the formation of the Ni—S bond was based on the assumption that the XANES peak change was due precisely to the Ni—S bond. XANES gives strong signal intensity but is not easily interpreted, while EXAFS gives much weaker signals, but can be analyzed based on single scattering theory to provide an easily interpreted local structure. Also XANES covers a narrow energy region of a few

electronic reprint

tens of electronvolts, while the EXAFS spectra cover a wide energy region of 600–1000 eV and require a long scanning time. There are two methods for acquiring time-resolved EXAFS (Newton *et al.*, 2002). One method is dispersive EXAFS (DEXAFS), which provides the whole EXAFS spectra at once using a bent crystal and a position-sensitive detector (Matsushita & Phizackerley, 1981; Pascarelli & Mathon, 2010). Although the acquisition time is potentially fast, it requires high sample homogeneity (Newton *et al.*, 2002). The other method is quick-EXAFS (QEXAFS), which is achieved by the fast scanning of the monochromator (Frahm, 1989; Dent, 2002; Oudenhuijzen *et al.*, 2002; Okumura *et al.*, 2007; Bando *et al.*, 2012). Since QEXAFS can use standard measurement equipment, it provides reliable data and is more tolerant of sample inhomogeneity. In this work we conducted QEXAFS measurements during the HDS reaction of thiophene. Problems with QEXAFS are low signal-to-noise ratio and the distortion of the EXAFS spectrum for the case that a structural change occurs in the time scale of a scan (Nomura, 2011). Since Ni EXAFS requires a measurement range of almost 800 eV and a high signal-to-noise ratio, each QEXAFS spectrum needs about 10 s for acquisition and the structure may change during the scan because the reaction time scale is a few minutes.

In this paper we propose a method of correction of transient EXAFS data up to second-order in time. We have compared the time dependence of *in situ* QEXAFS and XANES of Ni_2P/MCM-41 during the thiophene HDS reaction to find a direct correlation for the active site of Ni—S and the XANES changes. The good correlation between the measurements demonstrated that the Ni—S signal was not associated with deactivation or with adsorbed reaction intermediates but was related to the active site, supporting the formation of an active NiPS phase.

2. Experimental

2.1. Sample preparation

An MCM-41-supported Ni_2P catalyst was synthesized according to a previous report (Oyama *et al.*, 2004). The sample was reduced by temperature-programmed reduction in a flow of H_2 and was then passivated in a flow of 0.5% O_2/He for 4 h to prevent uncontrolled oxidation of the freshly produced phosphide. The loading of Ni was 1.16 mmol Ni $g^{-1}_{support}$. The sample was pressed into a disc and set at the center of an *in situ* cell (Bando *et al.*, 2012). The catalyst was activated in the cell under H_2 flow (100 ml min^{-1}) at 803 K for 2 h. Then the sample was cooled to HDS reaction temperatures in H_2 flow. The reaction was started by introduction of the reactant gas composed of thiophene (0.1 vol%), He (1.9 vol%) and H_2 (98 vol%) at a total flow rate of 100 ml min^{-1}.

2.2. *In situ* QEXAFS experiments

In situ QEXAFS measurements were mainly carried out at beamline 9C of the Photon Factory, the Institute of Materials Structure Science, High Energy Accelerator Research Organization. The ring energy and current were 2.5 GeV and 430 mA, respectively. The ring was operated in a top-up mode. A Si(111) double-crystal monochromator was rotated continuously to measure a whole EXAFS spectrum of 8900 eV in 10 s. The data were processed using *REX2000* (Rigaku) (Asakura, 1996). Curve-fitting analysis was performed using phase shift and amplitude functions derived from *FEFF8* (University of Washington) (Zabinsky *et al.*, 1995; Ankudinov *et al.*, 1998, 2002).

3. Results and discussion

3.1. Correction of QEXAFS during the scan

The observed QEXAFS spectrum, $\chi(k, t)$ can be expressed as shown in equation (1)

$$\chi(k, t) = c_1(t)\chi_1(k) + c_2(t)\chi_2(k) + c_3(t)\chi_3(k), \qquad (1)$$

where $\chi_1(k)$, $\chi_2(k)$, $\chi_3(k)$ are, respectively, the EXAFS oscillations of the catalyst before reaction, oscillations due to Ni—S appearing under the steady-state conditions, and oscillations of other components present only under transient conditions. Note that $\chi(k, t)$ has a time dependence while $\chi_1(k)$, $\chi_2(k)$, $\chi_3(k)$ are independent of time. Our previous work (Oyama *et al.*, 2004; Kawai *et al.*, 2006, 2008; Bando *et al.*, 2009) indicated that Ni—S bond formation occurs with the Ni_2P framework unchanged so that $c_1(t)$ is set constant and (1) can be reduced to

$$\chi(k, t) = \chi_1(k) + c_2(t)\chi_2(k) + c_3(t)\chi_3(k). \qquad (2)$$

The difference spectrum is described as

$$\Delta\chi(k, t) = \chi(k, t) - \chi_1(k) = c_2(t)\chi_2(k) + c_3(t)\chi_3(k). \qquad (3)$$

Under steady-state conditions, c_2 (t = steady state) = 1, c_3 (t = steady state) = 0. Thus the difference spectrum is expressed as $\Delta\chi(k, t$ = steady state) = $\chi_2(k)$. In the transient region $0 \le c_2(t) \le 1$, $c_3(t) \ge 0$.

If the time, τ, is measured from the origin of each nth run, t_n, then $t = t_n + \tau$, and $\chi(k,t)$ is expanded by τ at t_n,

$$\begin{aligned}\chi(k, t_n + \tau) &= \chi_1(k) + c_2(t_n + \tau)\chi_2(k) + c_3(t_n + \tau)\chi_3(k) \\ &\cong \chi_1(k) + \left[c_2(t_n) + c_2'(t_n)\tau + (1/2)c_2''(t_n)\tau^2\right]\chi_2(k) \\ &\quad + \left[c_3(t_n) + c_3'(t_n)\tau + (1/2)c_3''(t_n)\tau^2\right]\chi_3(k), \qquad (4)\end{aligned}$$

where $c_2'(t) = dc_2(t)/dt$, $c_3'(t) = dc_3(t)/dt$, $c_2''(t) = d^2c_2(t)/dt^2$, $c_3''(t) = d^2c_3(t)/dt^2$.

In order to obtain the first and second derivatives, differences of sequential spectra are taken,

electronic reprint

$$\begin{aligned}\delta\chi(k,t_n+\tau) &= \chi(k,t_{n+1}+\tau)-\chi(k,t_n+\tau)\\ &\cong \Big\{\big[c_2(t_{n+1})-c_2(t_n)\big]+\big[c_2'(t_{n+1})-c_2'(t_n)\big]\tau\\ &\quad +(1/2)\big[c_2''(t_{n+1})-c_2''(t_n)\big]\tau^2\Big\}\chi_2(k)\\ &\quad +\Big\{\big[c_3(t_{n+1})-c_3(t_n)\big]+\big[c_3'(t_{n+1})-c_3'(t_n)\big]\tau\\ &\quad +(1/2)\big[c_3''(t_{n+1})-c_3''(t_n)\big]\tau^2\Big\}\chi_3(k)\\ &\cong \big[c_2'(t_n)\delta t+(1/2)c_2''(t_n)(\delta t^2+2\delta t\tau)\big]\chi_2(k)\\ &\quad +\big[c_3'(t_n)\delta t+(1/2)c_3''(t_n)(\delta t^2+2\delta t\tau)\big]\chi_3(k)\\ &= \Big\{\big[c_2'(t_n)\chi_2(k)+c_3'(t_n)\chi_3(k)\big]\delta t\\ &\quad +(1/2)\big[c_2''(t_n)\chi_2(k)+c_3''(t_n)\chi_3(k)\big](\delta t^2+2\delta t\tau)\Big\},\end{aligned}$$

$$\begin{aligned}\delta\chi(k,t_{n-1}+\tau) &= \chi(k,t_n+\tau)-\chi(k,t_{n-1}+\tau)\\ &\cong \big[c_2'(t_n)\delta t+(1/2)c_2''(t_n)(-\delta t^2+2\delta t\tau)\big]\chi_2(k)\\ &\quad +\big[c_3'(t_n)\delta t+(1/2)c_3''(t_n)(-\delta t^2+2\delta t\tau)\big]\chi_3(k)\\ &= \big[c_2'(t_n)\chi_2(k)+c_3'(t_n)\chi_3(k)\big]\delta t\\ &\quad +\big\{(1/2)\big[c_2''(t_n)\chi_2(k)+c_3''(t_n)\chi_3(k)\big]\\ &\quad \times(-\delta t^2+2\delta t\tau)\big\},\end{aligned}$$

$$\begin{aligned}c_2''(t_n)\chi_2(k)+c_3''(t_n)\chi_3(k) =\\ \big[\delta\chi(k,t_n+\tau)-\delta\chi(k,t_{n-1}+\tau)\big]/\delta t^2,\end{aligned}\qquad(5)$$

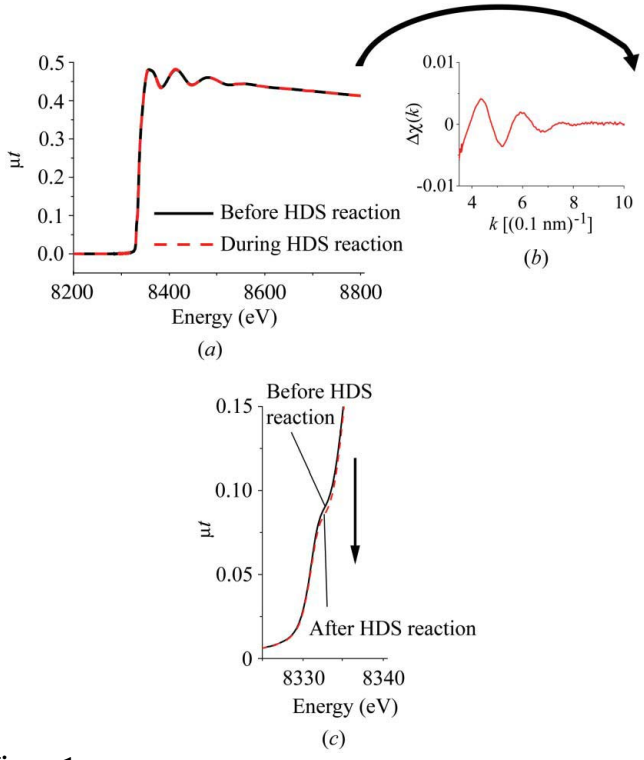

Figure 1
(*a*) XAFS oscillations before reaction (solid black line) and under steady-state reaction (broken red line). (*b*) Difference spectrum between the XAFS oscillations. (*c*) Expanded figure around the edge region before reaction (solid black line) and under steady-state reaction (broken red line).

$$\begin{aligned}c_2'(t_n)\chi_2(k)+c_3'(t_n)\chi_3(k) &= \frac{\delta\chi(k,t_n+\tau)}{\delta t}\\ &\quad -\frac{1}{2}\frac{\big[\delta\chi(k,t_n+\tau)-\delta\chi(k,t_{n-1}+\tau)\big]}{\delta t^2}(\delta t+2\tau)\\ &= \frac{1}{2}\left[\frac{\delta\chi(k,t_n+\tau)+\delta\chi(k,t_{n-1}+\tau)}{\delta t}\right]\\ &\quad -\frac{\big[\delta\chi(k,t_n+\tau)-\delta\chi(k,t_{n-1}+\tau)\big]}{\delta t}\frac{\tau}{\delta t},\end{aligned}\qquad(6)$$

where the third and higher derivatives are neglected. δt is the time difference between two sequential scans: $\delta t = t_{n+1} - t_n$.

Here a virtual difference spectrum $\delta\chi(k, t_n)$ is defined between two sequential spectra at time t_n and is approximated using (5) and (6),

$$\begin{aligned}\delta\chi(k,t_n) &= \chi(k,t_{n+1})-\chi(k,t_n)\\ &= \big[\chi_1(k)+c_2(t_{n+1})\chi_2(k)+c_3(t_{n+1})\chi_3(k)\big]\\ &\quad -\big[\chi_1(k)+c_2(t_n)\chi_2(k)+c_3(t_n)\chi_3(k)\big]\\ &= \big[c_2(t_{n+1})-c_2(t_n)\big]\chi_2(k)+\big[c_3(t_{n+1})-c_3(t_n)\big]\chi_3(k)\\ &\cong \big[c_2'(t_n)\delta t+(1/2)c_2''(t_n)\delta t^2\big]\chi_2(k)\\ &\quad +\big[c_3'(t_n)\delta t+(1/2)c_3''(t_n)\delta t^2\big]\chi_3(k)\\ &= \big[c_2'(t_n)\chi_2(k)+c_3'(t_n)\chi_3(k)\big]\delta t\\ &\quad +(1/2)\big[c_2''(t_n)\chi_2(k)+c_3''(t_n)\chi_3(k)\big]\delta t^2\\ &= (1/2)\big[\delta\chi(k,t_n+\tau)+\delta\chi(k,t_{n-1}+\tau)\big]\\ &\quad -\big[\delta\chi(k,t_n+\tau)-\delta\chi(k,t_{n-1}+\tau)\big]\big[(\tau/\delta t)-(1/2)\big].\end{aligned}\qquad(7)$$

Consequently the difference $\delta\chi(k, t_n) = \chi(k, t_{n+1}) - \chi(k, t_n)$ can be expressed as

$$\begin{aligned}\delta\chi(k,t_n) &= \delta\chi(k,t_n+\tau)\\ &\quad -\big[\delta\chi(k,t_n+\tau)-\delta\chi(k,t_{n-1}+\tau)\big]\frac{\tau}{\delta t}.\end{aligned}\qquad(8)$$

3.2. Difference spectrum of QEXAFS in the transient state

Fig. 1 shows the difference spectra of EXAFS, $\Delta\chi(k, t =$ steady state$) = \chi_2(k)$, *i.e.* the difference in spectra of the sample before reaction and under steady-state HDS conditions (reaction temperature = 559 K). The figure also shows the change in XANES spectra. The difference EXAFS spectrum yields a single sinusoidal curve as shown in Fig. 1(*b*). Curve-fitting analysis revealed the formation of Ni—S bonds with bond distance = 0.230 ± 0.003 nm and coordination number = 0.10 ± 0.02, as reported in previous work (Kawai *et al.*, 2006). There also appeared a shoulder at 8333.3 eV in the XANES spectrum before reaction as shown in Fig. 1(*c*). This feature decreased by 10% under steady-state conditions as shown by the dotted line. This small change was reproducible and could be used to follow changes in reaction by monitoring the intensity change in the XANES region as in previous work (Oyama *et al.*, 2009; Bando *et al.*, 2009, 2012).

Fig. 2 shows the $\delta\chi(k, t_n)$ data and the Fourier transforms. The data can be divided into four regions. In region I ($n = 1, 2$) $\delta\chi(k, t_n)$ gradually increases, in region II (n = 3–5) it is rela-

electronic reprint

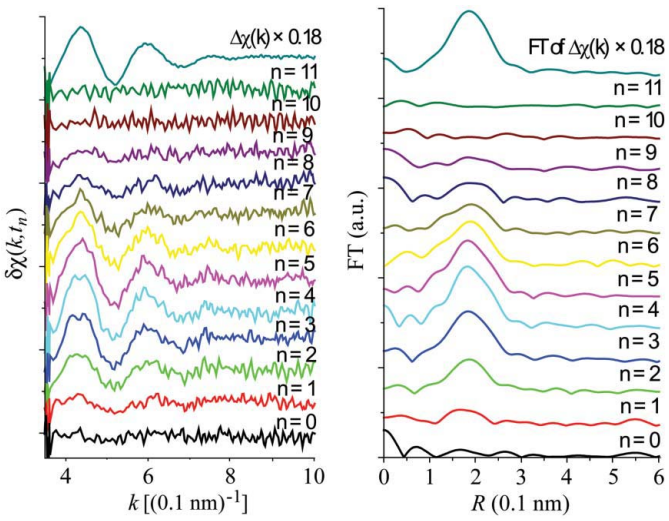

Figure 2
$\delta\chi(k, t_n)$ and their Fourier transforms. The difference spectrum between the spectra before reaction and under steady state $[\Delta\chi(k)]$ and its Fourier transform are given at the top.

tively constant, in region III (n = 6–8) it decreases, and in the steady-state region IV (n = 9–11) it shows no signal. The $\delta\chi(k, t_n)$ in region II (n = 3, 4, 5) can be described with only the first term in (8) because $\delta\chi(k, t_n) \cong \delta\chi(k, t_{n-1})$. The $\delta\chi(k, t_n)$ in region II has a similar shape to $\chi_2(k)$ within the limit of error, indicating a negligibly small contribution of $\chi_3(k)$.

Consequently using (6) and (7),

$$\delta\chi(k, t_n) = c_2'(t_n)\delta t\chi_2(k). \tag{9}$$

In regions I and III, $\delta\chi(k, t_n)$ showed little difference in oscillation from $\chi_2(k)$, indicating that the contribution of $\chi_3(k)$ was minimal. The $\chi_3(k)$ signal is expected to be due to the adsorption of thiophene. The lack of detection of a thiophene adsorbate in XANES could be due to thiophene being adsorbed very weakly or thiophene reacting very rapidly. It can be safely concluded that the main component in $\delta\chi(k, t_n)$ is proportional to $\chi_2(k)$ and to the number of Ni—S bonds.

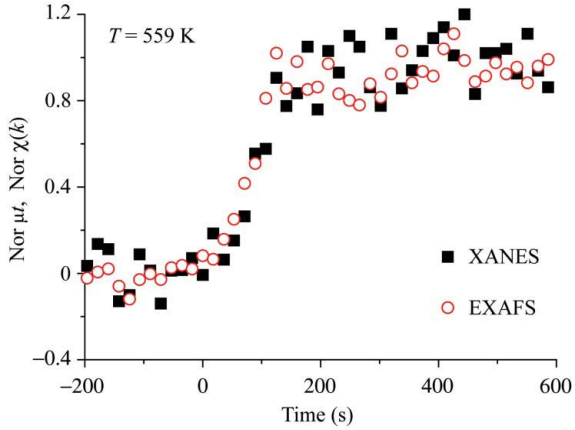

Figure 3
Time dependence of $\sum_{i=1}^{n}[c_2'(t_i)\delta t + (1/2)c_2''(t_i)\delta t^2]$ (open red circles) and XANES peak intensity (filled black squares).

The signal $\chi(k, t_n)$ can be reconstructed using $\delta\chi(k, t_i)$, the EXAFS oscillation, at time t_n as follows,

$$\chi(k, t_n) = \chi(k, t_0) + \sum_{i=1}^{n}\delta\chi(k, t_i), \tag{10}$$

$$\begin{aligned}\Delta\chi(k, t_n) &= \chi(k, t_n) - \chi(k, t_0)\\ &= \sum_{i=1}^{n}\delta\chi(k, t_i)\\ &= \left\{\sum_{i=1}^{n}\left[c_2'(t_i)\delta t + (1/2)c_2''(t_i)\delta t^2\right]\right\}\chi_2(k).\end{aligned} \tag{11}$$

Fig. 3 shows the time dependence of $\sum_{i=1}^{n}[c_2'(t_i)\delta t + (1/2)c_2''(t_i)\delta t^2]$ together with the intensity change in the XANES at 8333.3 eV. The two series of data points agree very well with each other. They also agree at different temperatures as shown in Fig. 1S of the supplementary material.[1] The occurrence of the same time-dependence indicates that the changes in the XANES and EXAFS signals have the same origin, *i.e.* the formation of Ni—S bonds. Combining the previous results of simultaneous XANES and products analysis (Bando *et al.*, 2009, 2012), the present paper demonstrates that the assumption that the XANES change is due to Ni—S formation is valid. Hence the Ni—S bond at 0.230 nm is involved in the active phase. The reaction activity is accelerated after the formation of sufficient Ni—S bonds, indicating that a Ni—S assemble is necessary for producing high activity (Bando *et al.*, 2009).

QEXAFS has many advantages compared with DEXAFS, although the latter is a much faster measurement: (i) QEXAFS is less affected by the inhomogeneity of the sample; (ii) QEXAFS covers a wide range with good energy resolution and sufficiently high speed; (iii) the sample and beamline set-up can be shared with normal EXAFS; (iv) QEXAFS can be used with other *in situ* detection techniques such as FTIR.

The difference spectrum method for sequential transient data using (8) will help to enhance the time resolution of QEXAFS with little distortion.

This work was supported by the US Department of Energy, Office of Basic Energy Sciences, through Grant DE-FG02-963414669, a JST Grant-in-Aid for Scientific Research (Category S, No. 16106010 and Category B, No. 16360405), and the Cooperative Research Program of Catalysis Research Center, Hokkaido University (Grant Nos. 10B1001, 10B2009 and 11B1018). The XAFS experiments were conducted under approval of PF-PAC (Project No. 2010G127, 2008G129, 2006G109) and partially conducted at BL14B2 at SPring-8 (2011A1972 as recovery support program from earthquake in JASRI). KKB was supported by the support program for earthquake recovery of the Catalysis Research Center, Hokkaido University #001.

[1] Supplementary data for this paper are available from the IUCr electronic archives (Reference: HI5626). Services for accessing these data are described at the back of the journal.

electronic reprint

References

Ankudinov, A. L., Ravel, B., Rehr, J. J. & Conradson, S. D. (1998). *Phys. Rev. B*, **58**, 7565–7576.

Ankudinov, A. L., Rehr, J. J., Low, J. J. & Bare, S. R. (2002). *Top. Catal.* **18**, 3–7.

Asakura, K. (1996). *X-ray Absorption Fine Structure for Catalysts and Surfaces*, Vol. 2, edited by Y. Iwasawa, pp. 33–58. Singapore: World Scientific.

Bando, K. K., Wada, T., Miyamoto, T., Miyazaki, K., Takakusagi, S., Gotto, T., Yamaguchi, A., Nomura, M., Oyama, S. T. & Asakura, K. (2009). *J. Phys. Conf. Ser.* **190**, 012158.

Bando, K. K., Wada, T., Miyamoto, T., Miyazaki, K., Takusagi, S., Koike, Y., Inada, Y., Nomura, M., Yamaguchi, A., Gott, T., Oyama, S. T. & Asakura, K. (2012). *J. Catal.* **286**, 165–171.

Bart, J. C. J. (1986). *Adv. Catal.* **34**, 203–296.

Bart, J. C. J. & Vlaic, G. (1987). *Adv. Catal.* **35**, 1–138.

Dent, A. J. (2002). *Top. Catal.* **18**, 27–35.

Dhandapani, B., Ramanathan, S., Yu, C. C., Fruhberger, B., Chen, J. G. & Oyama, S. T. (1998). *J. Catal.* **176**, 61–67.

Frahm, R. (1989). *Rev. Sci. Instrum.* **60**, 2515–2518.

Iwasawa, Y. (1996). Editor. *X-ray Absorption Fine Structure for Catalysts and Surfaces*, 1st ed. Singapore: World Scientific.

Kawai, T., Bando, K. K., Lee, Y.-K., Oyama, S. T., Chun, W.-J. & Asakura, K. (2006). *J. Catal.* **241**, 20–24.

Kawai, T., Bando, K. K., Lee, Y.-K., Oyama, S. T., Chun, W.-J. & Asakura, K. (2007). *AIP Conf. Proc.* **882**, 616–618.

Kawai, T., Chun, W. J., Asakura, K., Koike, Y., Nomura, M., Bando, K. K., Ted Oyama, S. & Sumiya, H. (2008). *Rev. Sci. Instrum.* **79**, 014101.

Kim, J. H., Ma, X., Song, C., Lee, Y.-K. & Oyama, S. T. (2005). *Energy Fuels*, **19**, 353–364.

Matsushita, T. & Phizackerley, R. P. (1981). *J. App. Chem.* **20**, 2223–2228.

Newton, M. A., Dent, A. J. & Evans, J. (2002). *Chem. Soc. Rev.* **31**, 83–95.

Nomura, M. (2011). *Acta Cryst.* A**67**, C172.

Okumura, K., Kato, K., Sanada, T. & Niwa, M. (2007). *J. Phys. Chem. C*, **111**, 14426–14432.

Oudenhuijzen, M. K., Kooyman, P. J., Tappel, B., van Bokhoven, J. A. & Koningsberger, D. C. (2002). *J. Catal.* **205**, 135–146.

Oyama, S. T. (2003). *J. Catal.* **216**, 343–352.

Oyama, S. T., Gott, T., Asakura, K., Takakusagi, S., Miyazaki, K., Koike, Y. & Bando, K. K. (2009). *J. Catal.* **268**, 209–222.

Oyama, S. T., Wang, X., Lee, Y. K., Bando, K. & Requejo, F. G. (2002). *J. Catal.* **210**, 207–217.

Oyama, S. T., Wang, X., Lee, Y.-K. & Chun, W.-J. (2004). *J. Catal.* **221**, 263–273.

Pascarelli, S. & Mathon, O. (2010). *Phys. Chem. Chem. Phys.* **12**, 5535–5546.

Sawhill, S. J., Layman, K. A., Van Wyk, D. R., Engelhard, M. H., Wang, C. & Bussel, M. E. (2005). *J. Catal.* **231**, 300–313.

Zabinsky, S. I., Rehr, J. J., Ankudinov, A., Albers, R. C. & Eller, M. J. (1995). *Phys. Rev. B*, **52**, 2995–3009.

electronic reprint